molecular human reproduction

ORIGINAL RESEARCH

Genome-wide DNA methylation identifies trophoblast invasion-related genes: Claudin-4 and Fucosyltransferase IV control mobility via altering matrix metalloproteinase activity

Yuxiang Hu[1,2], John D. Blair[2,3], Ryan K.C. Yuen[4], Wendy P. Robinson[2,3], and Peter von Dadelszen[1,2,*]

[1]Department of Obstetrics and Gynaecology, University of British Columbia, Vancouver, BC, Canada [2]Child and Family Research Institute, University of British Columbia, Vancouver, BC, Canada [3]Department of Medical Genetics, University of British Columbia, Vancouver, BC, Canada [4]Genetics and Genome Biology, The Hospital for Sick Children, Toronto, ON, Canada

*Correspondence address. Division of Maternal Fetal Medicine, Department of Obstetrics and Gynaecology, University of British Columbia, Clinical Services Building, Room V3-339, 950 West 28th Avenue, Vancouver, BC V5Z 4H4, Canada. E-mail: pvd@cw.bc.ca

ABSTRACT: Previously we showed that extravillous cytotrophoblast (EVT) outgrowth and migration on a collagen gel explant model were affected by exposure to decidual natural killer cells (dNK). This study investigates the molecular causes behind this phenomenon. Genome wide DNA methylation of exposed and unexposed EVT was assessed using the Illumina Infinium HumanMethylation450 BeadChip array (450 K array). We identified 444 differentially methylated CpG loci in dNK-treated EVT compared with medium control ($P < 0.05$). The genes associated with these loci had critical biological roles in cellular development, cellular growth and proliferation, cell signaling, cellular assembly and organization by Ingenuity Pathway Analysis (IPA). Furthermore, 23 mobility-related genes were identified by IPA from dNK-treated EVT. Among these genes, *CLDN4* (encoding claudin-4) and *FUT4* (encoding fucosyltransferase IV) were chosen for follow-up studies because of their biological relevance from research on tumor cells. The results showed that the mRNA and protein expressions of both *CLDN4* and *FUT4* in dNK-treated EVT were significantly reduced compared with control ($P < 0.01$ for both *CLDN4* and *FUT4* mRNA expression; $P < 0.001$ for *CLDN4* and $P < 0.01$ for *FUT4* protein expression), and were inversely correlated with DNA methylation. Knocking down *CLDN4* and *FUT4* by small interfering RNA reduced trophoblast invasion, possibly through the altered matrix metalloproteinase (MMP)-2 and/or MMP-9 expression and activity. Taken together, dNK alter EVT mobility at least partially in association with an alteration of DNA methylation profile. Hypermethylation of *CLDN4* and *FUT4* reduces protein expression. *CLDN4* and *FUT4* are representative genes that participate in modulating trophoblast mobility.

Key words: Claudin-4 / decidual natural killer cells / DNA methylation / extravillous cytotrophoblast / Fucosyltransferase IV

Introduction

Cytotrophoblasts display strong mobility and invasiveness while differentiating into extravillous trophoblasts (EVT) during implantation and placentation. EVT penetrate the decidua and the inner third of the myometrium where they replace endothelial cells to remodel spiral arteries. This process is regulated by maternal immune cells, growth factors, extracellular matrix components and adhesion molecules at the fetal–maternal interface (Damsky *et al.*, 1992; Knofler, 2010; Wallace *et al.*, 2012). The functional change in EVT is accompanied by the alteration of gene expression (Burrows *et al*, 1996; Fukushima *et al.*, 2005). The gene expression

alteration in EVT may be associated with epigenetic modification, as well as transcriptional, post-transcriptional and translational regulation.

Immune cells and the maternal–fetal interface play an important role in the regulation of implantation and placentation. A subset of natural killer cells (NK) expressing CD56^{bright}/CD16^{-} are the dominant immune cells in the decidua during the first trimester of pregnancy, and interact directly with EVT. The decidual NK (dNK) cells exert lower cytotoxic but higher secretory capacity compared with peripheral NK cells (Hanna *et al.*, 2006; Yagel, 2009; Wallace *et al.*, 2012). Evidence from our own and other studies demonstrates that dNK regulate EVT migration and invasion through secreted soluble growth factors such as

transforming growth factor-beta (TGF-β1 and TGF-β2) (Clark et al., 1994; Karmakar and Das, 2002; Lash et al., 2006); chemokines such as interleukin (IL)-8 and interferon gamma inducible protein-10 (IP-10) (Hanna et al., 2006); and cytokines such as IL-6, IL-10, interferon (IFN)-γ and tumor necrosis factor (TNF)-α (Vigano et al., 2001; Hu et al., 2006, 2008; Eastabrook et al., 2008; Pitman et al., 2013). Among these factors, TGF-β1, TGF-β2, IL-10, IFN-γ and TNF-α potentially restrict EVT migration and invasion (Clark et al., 1994; Lash et al., 2005; Hu et al., 2006, 2008; Pang et al., 2008); while other factors like IL-8 and IP-10 were reported to promote EVT migration and invasion (Hanna et al., 2006). What has not yet been shown is the mechanisms by which the behavior of EVT is altered upon interacting with dNK.

DNA methylation is an epigenetic modification which plays a role in programmed gene regulation during cellular differentiation as well as adaptation to environmental conditions. DNA methylation occurs almost exclusively at CpG dinucleotides, and is commonly associated with altered gene expression (Mohtat and Susztak, 2010; Hamilton, 2011). Widespread changes in DNA methylation are found in placentas associated with pregnancy complications such as pre-eclampsia (Yuen et al., 2010; Blair et al., 2013). Alterations in DNA methylation have also been observed in cytotrophoblasts exposed to varying oxygen tensions (Yuen et al., 2013).

Our previous study investigated the interaction of dNK and EVT cells using an ex-vivo first trimester villous explant culture on collagen gel (Hu et al., 2006). We found that EVT underwent outgrowth, column formation and then migration from the anchoring villous tips when cultured alone or with IL-15 (used to support dNK proliferation and survival). By co-culturing explants with either dNK directly or dNK trapped inside a hollow fiber (HF-dNK), the EVT outgrowth pattern was altered and EVT migration appeared to be restricted by both dNK and HF-dNK. The phenotypic changes in EVT were associated with changes in protein expression, including matrix metalloproteases-2 and -9 (MMP-2 and MMP-9) and plasminogen activator inhibitor-1.

In the current study, we examined whether or not dNK-induced EVT phenotypic alterations were associated with changes of DNA methylation. Whole genome DNA methylation was surveyed using the Infinium HumanMethylation450 BeadChip array (450 K array). The network composition and bio-functional analysis by ingenuity pathway analysis (IPA) software identified molecular pathways and gene sets associated with cellular development, growth and proliferation, signaling, organization and maintenance, and notably, with cellular movement. We hypothesized that the methylation alteration of cellular movement genes by dNK might influence gene expression, leading to the changes of cellular behaviors including migration and invasion, the phenomenon we observed previously (Hu et al., 2006). Hence, the confirmation of methylation, gene expression analysis and gene functional assessment were focused on two candidate genes [CLDN4 (encoding Claudin-4 protein or CLDN4) and FUT4 (encoding Fucosyltransferase IV protein or FUT4)] from an IPA identified gene set associated with cellular movement.

Materials and Methods

Preparation of dNK, HF-dNK and first-trimester villous explant culture

Placental tissues were collected from healthy women undergoing elective pregnancy termination at gestational ages of 7–9 weeks with ethical approval from the University of British Columbia and BC Children's and Women's Hospital ethics boards. Written informed consent was obtained from all women. dNK isolation, HF-dNK preparation and placental villous explant culture in rat-tail collagen were described previously (Hu et al., 2006, 2008). In brief, dNK were isolated from decidua after collagenase and hyaluronidase digestion and depletion of attached cells. They were then enriched using a human NK cell enrichment cocktail following the manufacturer's instructions (StemCell Technologies, Inc., Vancouver, Canada). The percentage of CD56$^+$/CD16$^-$ dNK reached ∼87%, while CD16$^+$ cells were <2.1% (Hu et al., 2006). The dNK were trapped inside a hollow fiber (Spectrum Laboratories, Inc., Rancho Dominquez, CA, USA) (HF-dNK) and used for co-culturing with explants in order to eliminate trophoblast cell contamination from dNK when performing EVT DNA extraction. The HF permits soluble factors with molecular weight below 500 kDa to be exchanged freely. For each placental specimen, villous explant cultures were set up in 12 well plates on collagen gel. After overnight incubation, explant cultures were exposed to medium control (Dulbecco's modified Eagle's medium/F12 supplemented with 10% fetal bovine serum (FBS)), or medium plus IL-15, or concordant HF-dNK plus IL-15, for a total of 96 h. In the whole study 'HF-dNK' refers to HF-dNK plus IL-15. We used 6–8 explants for each treatment group in each placental specimen. During the incubation, EVT moved out from the villous tips and expanded over the collagen gel. They migrated in a radially oriented direction especially from the edge of the column in the presence of medium control or medium plus IL-15, or were highly packed, especially around the edge of the column in the presence of HF-dNK (Hu et al., 2006).

DNA extraction of EVT from explant cultures

For each of the explant cultures, EVT were harvested from collagen gel after dissecting out villous tissue and pooled for each treatment group. Previous work has shown that the EVT harvested from collagen gel were cytokeratin positive and vimentin negative cells and purity was high (Hu et al., 2006, 2008). Genomic DNA from EVT was purified using the QIAamp DNA mini kit according to the manufacturer's instructions (Qiagen, Inc., Mississauga, ON, Canada). Five placental specimens in total were used for the global DNA methylation array and Bisulfite pyrosequencing validation.

Illumina HumanMethylation450 array

DNA samples were run on the Illumina HumanMethylation450 BeadChip (Illumina, Inc., San Diego, CA, USA) (450 K array) as described (Blair et al., 2013; Yuen et al., 2013). This array quantifies methylation at >480 000 cytosine-guanine dinucleotide (CpG) sites in 99% of RefSeq genes. Briefly, 750 ng of DNA was bisulfite converted using EZ DNA Methylation Kit (Zymo Research, Irvine, CA, USA). Hybridization of samples was performed following the manufacturer's protocol. Each chip was scanned by a HiScan 2000 (Illumina). Raw data were extracted into GenomeStudio (Illumina) and was subject to (i) background subtraction; and (ii) elimination of probes with detection P-value >0.01. In R, measurements were converted to an M-value (log^2 ratio of the intensities of methylated to unmethylated probes), color channel corrected and normalized using sub-quantile within array normalization. Candidate sites were prioritized by (i) P-value <0.05 and (ii) the magnitude of mean difference >10% (i.e. $\Delta\beta > 0.10$) between control group and sample group. Raw and processed data were deposited into the public database GEO (ncbi.nlm.nih.gov/geo/; GSE60885).

DNA methylation confirmation by bisulfite pyrosequencing

DNA methylation of selected candidate genes CLDN4 and FUT4 was confirmed using bisulfite pyrosequencing as described (Yuen et al., 2013). Assays were designed using PSQ Assay design (Biotage, Upsalsa, Sweden).

Methylation-unbiased pyrosequencing primers were designed to include the same CpG sites interrogated by the Illumina probes. The assay was run on a Qiagen Pyromark Q96 MD (Qiagen, Heiden, Germany). The quantitative levels of methylation for the CpG dinucleotide were evaluated with the Pyro Q-CpG software (Biotage, Uppsala, Sweden). The methylation level detected by pyrosequencing was concordant to that of the 450 k array ($R = 0.65$ for the *FUT4* and 0.61 for the *CLDN4* associated CpGs).

Gene network and pathway analysis

IPA (Ingenuity Systems, Redwood City, CA, USA) was used to carry out analyses for network composition and molecular and cellular functions for differentially methylated CpGs across various gene regions in HF-dNK-treated EVT cells. Each gene symbol was mapped to its corresponding gene object in the Ingenuity Pathways Knowledge Base. Networks of these genes were algorithmically generated based on their connectivity and assigned a score. The score is a numerical value used to rank networks according to how relevant they are to the genes in the input dataset but may not be an indication of the quality or significance of the network. The network identified is then presented as a graph indicating the molecular relationships between genes/gene products. The over-represented cellular and molecular functions were ranked according to the calculated *P*-value.

Flow cytometer

We performed cytometric analysis (FACScan flow cytometer, Beckton Dickinson, Oakville, ON, Canada) for CLDN4 and FUT4 protein expression level in EVT harvested from villous explants as described (Hu *et al.*, 2006, 2008). The data were generated from five placental specimens. In brief, villi were dissected from explant cultures, EVT were collected from collagen gel after treating with 0.25% EDTA and pooled from each treatment group. EVT were then fixed by adding 37% formaldehyde solution directly into cell suspension to obtain a final concentration of 1.5% formaldehyde. Cells were incubated for 20 min and pellets were collected by centrifugation at 300g for 5 min. Cells were then permeabilized by 100% ice-cold methanol for 5 min. Following permeabilization, cells were stained with Alexa Fluor 488-conjugated mouse anti-Claudin4 (Clone 3E2C1, Invitrogen, Frederick, MD 21704, USA) or rabbit anti-human FUT4 (sc-292247, Santa Cruz Biotechnology, Inc., Santa Cruz, CA 95060, USA) followed by fluorescein isothiocyanate labeled goat anti-rabbit immunoglobulin (Ig).

Total RNA preparation, first-strand cDNA synthesis and qPCR

Villi were removed from each explant culture. EVT were lysed and pooled from the same assay group and total RNA was prepared using RNeasy plus Mini kit according to the manufacturer's protocol (Qiagen, Inc., Mississauga, ON, Canada) as described previously (Hu *et al.*, 2006). Additionally, total RNA was prepared from HTR8/SVneo cells for *CLDN4* siRNA and *FUT4* small interfering (si)RNA knocking down efficiency test. The cDNA synthesis was performed using SuperScript III first-strand Synthesis SuperMix kit (Invitrogen, Burlington, ON, Canada) and quantitative PCR (qPCR) was performed in an ABI prism 7300 Sequence Detection System (Applied Biosystems, Foster City, CA, USA). After 2 min at 50°C and 10 min at 95°C the samples were cycled 40 times at 95°C for 15 s and 60°C for 60 s. The relative quantification of gene expression was calculated using glyceraldehyde-3-phosphate dehydrogenase (GAPDH) and β-actin (ACTB) gene expression as endogenous controls, as described (Hu *et al.*, 2006) and presented as relative expression in EVT in treated groups compared with medium control group. The primer sequences (all 5′ to 3′) and their Genebank accession numbers were as follows: *GAPDH* (NM_002046): forward: ATGGAAATCCCATCACCATCTT; Reverse: CGC CCCACTTGATTTTGG *ACTB* (NM_001101.3): forward: ATGATGATATCG CCGCGCTC; reverse: CCACCATCACGCCCTGG; bone morphogenetic

protein 4 (*BMP4*)(NM_130850.2): forward: CCCGGAAGCTAGGAGCCA TT; Reverse: AACGACCATCAGCATTCGGT; *CLDN4* (NM_001305): Forward: GCTGGCCAGGATAGCTTAACC; Reverse: GCCAACGCCGAT GCA; fibroblast growth factor receptor 3 (*FGFR3*)(NM_000142): forward: GTGACAGACGCTCCATCCTC; reverse: AGCTTCTTGTCCATCCGCTC; *FUT4* (NM_002033): Forward: TTGGGCTCCTGCACACAGT; Reverse: GGT GCTGCGAGTTCTCGA; interleukin-18 (*IL-18*) (NM_001562): forward: CTG CCACCTGCTGCAGTCT; reverse: TCTGGAAGGTCTGAGGTTCCT; integrin, beta 7 (*ITGB7*) (NM_000889): forward: TGCACGCACCTATGTGGAAA; reverse: TCCCAAGCCGTAGTGGTAGA; janus kinase 3 (*JAK3*) (NM_ 000215): forward: CATGGAGTCATTCCTGGAAGC; reverse: GGTGTACA AATTCCTGCACCAT; protein kinase, cAMP-dependent, regulatory, type I, beta (*PRKAR1B*) (NM_001164759): forward: TGTTCCCTGTCACTCACAT CG; reverse: CGTACACATCCACTTCCCCTT; phosphatidylinositol 4-phosphate 5-kinase, type-1, gamma (*PIP5K1C*) (NM_012398): forward: CCCGC CACCGACATCTAC; reverse: CTGCATAGAAATTATGTGTCGCTCT and thyroid hormone receptor interactor 6 (*TRIP6*) (NM_003302.2): forward: CC CTGCAGGAAGAGGAAGAG); reverse: CACACTGGCCAAAGTACTCCC.

Knockdown of *CLDN4* and *FUT4* by siRNA in HTR8/SVneo, immunocytochemistry staining and western blot

The X-tremeGENE siRNA transfection reagent (Roche, Basel, Switzerland) was used for siRNA transfection (Eastabrook *et al.*, 2012). Human siGEN-OME *CLDN4* siRNA SMARTpool, ON-TARGET plus *FUT4* smart pool siRNA and non-targeting control siRNA were purchased from Dharmacon, Thermo Fisher Scientific Biosciences (Lafayette, CO, USA). After transfection efficiency optimization, HTR8/SVneo cells were transfected with 50 nM, 12 nM and 3 nM *CLDN4* siRNA, *FUT4* siRNA or control siRNA. The co-transfection of *CLDN4* and *FUT4* at 3 concentrations was also carried out. At 72–96 h after transfection, the *CLDN4* and *FUT4* siRNA single and/or co-transfected cells were used for immunocytochemistry staining, western blot and/or invasion assay.

Immunocytochemistry staining: *CLDN4*, *FUT4* and control siRNA transfected HTR8/SVneo cells were seeded on cover slips. After overnight incubation, cells were fixed with ice-cold methanol, then blocked with phosphate-buffered saline (PBS) supplemented with 10% FBS and exposed to primary rabbit polyclonal anti-CLDN4 (sc-17664-R, Santa Cruz Biotechnology) or rabbit polyclonal anti-Fut4 antibody (sc-292247) at 2 μg/ml concentration overnight at 4°C. Cells were washed before exposing to Alexa Fluor 594-conjugated goat anti-rabbit IgG antibody (Life technology). The cover slips were mounted with Prolong gold antifade reagent with 4′,6-Diamidino-2-phenylindole (DAPI, Life technology).

Western Blot: The siRNA transfected HTR8/SVneo cells were lysed and underwent the procedures for western blot as described previously (Hu *et al.*, 2010). The primary rabbit polyclonal anti-CLDN4 (sc-17664-R, Santa Cruz Biotechnology) and rabbit polyclonal anti-Fut4 antibody (sc-292247) were used for the detection of CLDN4 and FUT4 protein expression.

Invasion assay

HTR8/SVneo invasion assays were performed in 24 well format 8 μm transwell inserts with polyethylene terephthalate track-etched membranes (Becton Dickinson, Franklin Lakes, NJ, USA) (Hu *et al.*, 2010). The inserts were coated with growth factor reduced Matrigel (BD Biosciences, Bedford, MA 01730, USA). Briefly, *CLDN4, FUT4* and control siRNA transfected cells were harvested and washed with PBS. Cells (2×10^5) in 0.1% FBS containing RPMI1640 media were loaded onto the top of the inserts. RPMI1640 containing 10% FBS was added to the bottom of the inserts. After overnight incubation, the inserts were transferred to new plates that

contained 225 μl of a 0.25% trypsin solution. The plate was incubated with shaking for 20 min. The inserts were then discarded and cells were stained with DNA dye CyQuant solution in lysis buffer (Molecular Probes, Invitrogen) for 20 min. Following that, 200 μl of cell mixture from a 24 well plate were transferred into a 96 well plate and the fluorescence was read with a fluorescent plate reader at 480 nm excitation and 520 nm emission. The results were expressed as % of control [% of control = (relative fluorescence units (RFU) in assay group − background) * 100/(RFU in control

Figure 1 Venn diagram summary of differentially methylated loci from interleukin (IL)-15 and Hollow fiber-decidual natural killer cells (HF-dNK)-treated extravillous cytotrophoblast (EVT). HF-dNK treatment on EVT resulted in 444 candidate loci with methylation alteration compared with medium control, and among them, there were 5 loci in common with IL-15 treated EVT. Number of differentially methylated loci is indicated in the circles. ↑: hypermethylated; ↓: hypomethylated.

siRNA group − background)]. Each assay was repeated for a total of four times.

Total and active MMP-2 and MMP-9 activity assessment

Following *CLDN4* and *FUT4* siRNA knock down in HTR8/SVneo cells, the supernatants were collected at 72 h and used for total and active MMP-2 and MMP-9 activity measurement using MMP-2 and MMP-9 Biotrak Activity Assay System (GE Healthcare, Amersham Place, Little Chalfont, Buckinghamshire, UK) (Hu *et al.*, 2006). The results were presented as % of control [% of control = (MMP level in assay siRNA group-background) *100/(MMP level in control siRNA group-background). Each assay was repeated for a total of five times.

Statistics

Data are presented as mean ± SD. Groups were compared with analysis of variance (ANOVA). When ANOVA showed a significant difference for the groups ($P < 0.05$), then post test was performed with Bonferroni comparison or Dunn's multiple comparison, as appropriate, using GraphPad Prism 4.0 software (San Diego, CA, USA). For the 450 k array, statistical significance was determined using Student's *T*-test with *P*-value cut-off set at $P < 0.05$.

Results

Genome-wide DNA methylation of explant culture-derived EVT

The 450 k array was used to evaluate genome-wide DNA methylation of EVT exposed to medium control, IL-15, and HF-dNK. Each group included five different placental specimens. To determine visually the relationship of samples with each other, two dimensional principal component analyses was used (Supplementary Fig. S1). As expected, samples clustered by the placenta of origin rather than by treatment, suggesting that genetic effects on the DNA methylome were the main source of variance among samples.
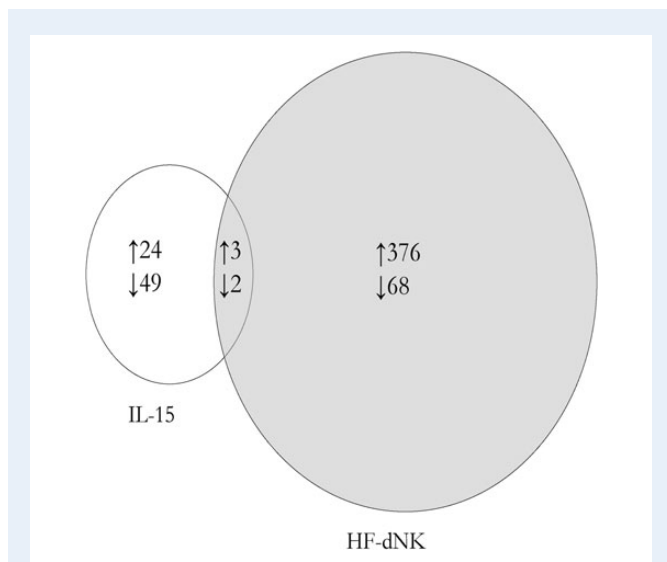
Table I Core ingenuity pathway analysis (IPA) of differentially methylated CpGs across gene regions from HF-dNK-treated extravillous cytotrophoblast (EVT) compared with control EVT.

Top networks—associated network functions		Score
Gene expression, organismal survival, cancer		44
Cell morphology, embryonic development, organismal development		39
Auditory and vestibular system development and function, cellular development, organ development		30
Cellular assembly and organization, connective tissue disorders, developmental disorder		30
Cell-to-cell signaling and interaction, nervous system development and function, cell death and survival		24
Top bio functions—molecular and cellular functions	**P-value**	**Number of molecules**
Cellular movement	1.20E-04 to 2.12E-02	23
Cellular development	2.78E-04 to 4.39E-02	32
Cellular growth and proliferation	9.41E-04 to 4.39E-02	28
Cell signaling	1.24E-03 to 2.51E-02	40
Cellular assembly and organization	1.56E-03 to 3.75E-02	19

HF-dNK: hollow fiber-decidual natural killer cells.

Alteration of EVT DNA methylation by exposing to HF-dNK

No loci were significant using a false discovery rate (FDR) analysis which corrects for multiple comparisons. However, using a cut-off of $P < 0.05$ and $>10\%$ absolute average methylation difference ($\Delta\beta > 0.1$ from 450 k array) before and after treatment, we identified 73 (24 hypermethylated; 49 hypomethylated) and 444 (376 hypermethylated; 68 hypomethylated) candidate methylation changes in IL-15 and HF-dNK-treated EVT, respectively, compared with medium control. Hence the NK treatment appeared to have a greater effect on EVT DNA methylation than the IL-15 treatment. Of the 73 loci altered with IL-15 treatment, 5 CpGs

(representing 5 genes) were in common with those altered in HF-dNK-treated (0.09%) EVT, indicating that there may be a minimal overlap in effect (Fig. 1). Subsequent analysis was focused on candidates derived from HF-dNK-treated EVT. The genomic sequence from 200 bp downstream to 200 bp upstream surrounding each significant CpG from HF-dNK-treated EVT was interrogated for recurring DNA motifs and none were found to be significant.

IPA of DNA methylation changes

To identify pathways and functional groups enriched by differentially methylated loci in HF-dNK-treated EVT, the 444 CpG loci with altered
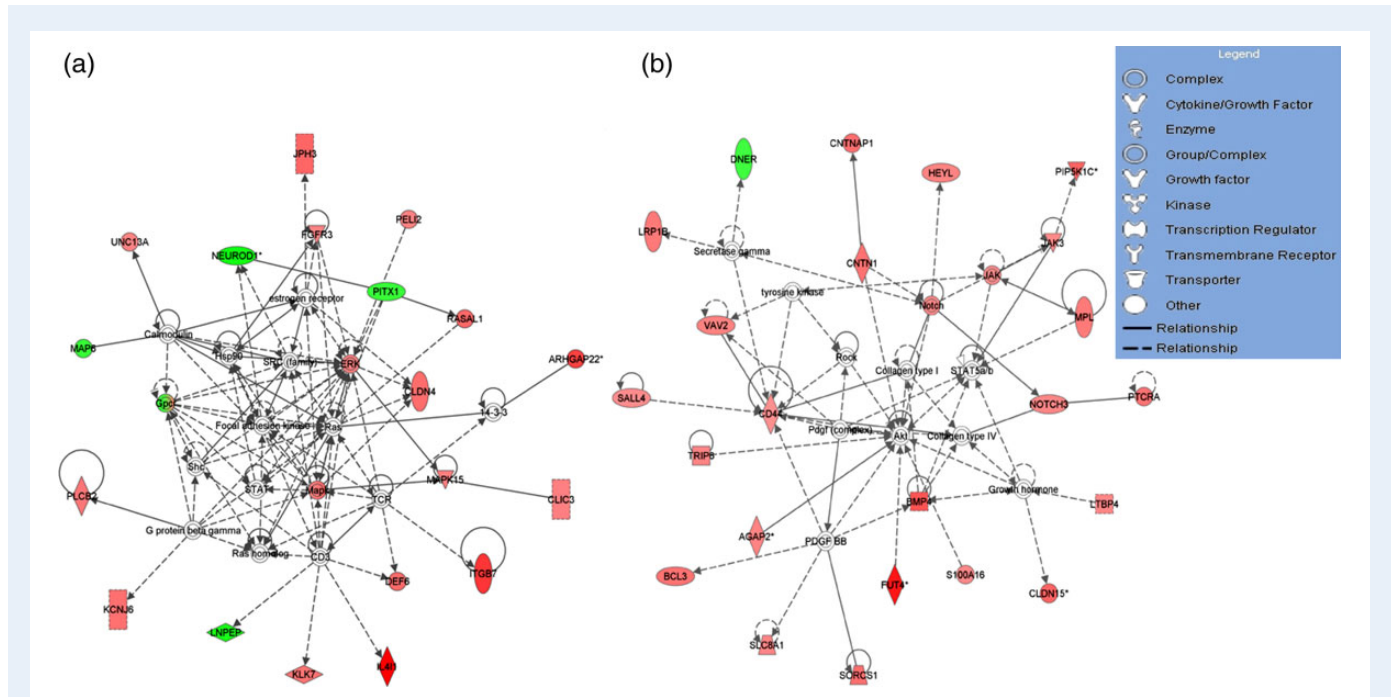

Figure 2 The two representative networks by ingenuity pathway analysis (IPA) for differentially methylated whole gene set derived from HF-dNK-treated EVT. (**a**) Extracellular signal-regulated protein kinase 1 and 2 (Erk1/2) was centered in one of the top network pathways, and Claudin-4 (CLDN4) was revolved this pathway. (**b**) Protein kinase B (AKT) was centered in another top network pathway, and fucosyltransferase IV (FUT4) was revolved this pathway. The analyses indicate that the differentially methylated genes from HF-dNK-treated EVT are located in pathways related to cellular development, cellular function and maintenance, and cell-to-cell signaling and interaction, revolving around key cellular proteins AKT and Erk1/2. The color intensity of node indicates the degree of hyper- or hypo-methylation. Genes encoding for molecules in red are hypermethylated while those in green are hypomethylated relative to control EVT. The shape of each node denotes the molecule class displayed beside each figure. The nodal relationships indicated in solid lines denote direct while those in dashed lines denote indirect interactions. AGAP2: ArfGAP with GTPase domain, ankyrin repeat and PH domain 2; ARC: Activity-regulated cytoskeleton-associated protein; BCL3: B cell lymphoma 3 protein; BMP4: bone morphogenetic protein 4; CD3: cluster of differentiation 3; CD44: cluster of differentiation 44; CLIC3: chloride intracellular channel 3; CNTN1: contactin 1; CNTNAP1: contactin associated protein 1; DEF6: differentially expressed in FDCP 6 homolog; DNER: delta and notch-like epidermal growth factor-related receptor; FGFR3: fibroblast growth factor receptor 3; GPC1: glypican 1; HEYL: hes-related family bHLH transcription factor with YRPW motif-like; Hsp90: 90 kDa heat shock protein; IL4I1: interleukin 4 induced 1; ITGB7: intergrin, beta 7; JAK: janus kinase; JAK3: janus kinase 3; KCNJ6: potassium inwardly-rectifying channel, subfamily J, member 6; KLK7: kallikrein-related peptidase 7; LNPEP: leucyl/cystinyl aminopeptidase; LRP1B: low density lipoprotein receptor-related protein 1B; MAP6: microtubule-associated protein 6; MAPK: mitogen-activated protein kinase; MPL: myeloproliferative leukemia virus oncogene; NEUROD1: neuronal differentiation 1; NOTCH3: Notch homolog 3; PDGF BB: platelet-derived growth factor beta polypeptide homodimer; PELI2: pellino E3 ubiquitin protein ligase family member 2; PIP5K1C: phosphatidylinositol-4-phosphate 5-kinase, type I, gamma; PITX1: paired-like homeodomain 1; PLCB2: phospholipase C, beta 2; PTCRA: pre T-cell antigen receptor alpha; RASAL1: RAS protein activator like 1; ROCK: rho-associated, coiled-coil-containing protein kinase; S100A16: S100 calcium binding protein A16; SALL4: spalt-like transcription factor 4; Shc: SHC (Src homology 2 domain containing) transforming protein; SLC8A1: solute carrier family 8 (sodium/calcium exchanger), member 1; SORCS1: sortilin-related VPS10 domain containing receptor 1; STAT: signal transducer and activator of transcription; STAT5a/b: signal transducer and activator of transcription 5a/b; TCR: T cell receptor; TRIP6: thyroid hormone receptor interactor 6; UNC13A: protein unc-13 homolog A; VAV2: vav 2 guanine nucleotide exchange factor.

Table II List of differentially methylated genes overrepresented with cellular movement identified by IPA.

UCSC_RefGene_Name	CHR	UCSC_RefGene_Accession	UCSC_RefGene_Group	Enhancer	Δβ*	P-value
FUT4	11	NM_002033	1st Exon	TRUE	0.1357	0.0000
ITGB7	12	NM_000889	Body		0.1622	0.0003
PRKAR1B	7	NM_001164759	Body		0.1125	0.0007
TRIP6	7	NM_003302	Body		0.1091	0.0013
SPI1	11	NM_001080547	3'UTR	TRUE	0.1068	0.0014
PLCB2	15	NM_004573	Body	TRUE	0.1103	0.0018
IL18	11	NM_001562	TSS200		−0.1117**	0.0019
SH2D3C	9	NM_005489	Body; 5'UTR		0.1227	0.0021
MAPK10	4	NM_138980	5'UTR	TRUE	0.1320	0.0034
CLDN4	7	NM_001305	1st Exon	TRUE	0.1184	0.0060
STAB1	3	NM_015136	Body	TRUE	0.1012	0.0061
PGLYRP2	19	NM_052890	Body		0.1363	0.0078
CHAT	10	NM_001142929	1st Exon	TRUE	−0.1100	0.0111
MAP4K1	19	NM_001042600	Body		0.1534	0.0114
FGFR3	4	NM_001163213	Body		0.1010	0.0129
FRZB	4	NM_001463	5'UTR; 1st Exon	TRUE	−0.1031	0.0132
AIRE	21	NM_000383	TSS200		0.1115	0.0134
ETS1	11	NM_001143820	Body	TRUE	0.1198	0.0203
PIP5K1C	19	NM_012398	Body		0.1270	0.0236
BMP4	14	NM_130850	Body		0.1529	0.0263
JAK3	19	NM_000215	Body	TRUE	0.1047	0.0316
RIMS1	6	NM_001168407	TSS200; Body		−0.1357	0.0327
CD44	11	NM_001001391	TSS1500		0.1010	0.0494

AIRE: autoimmune regulator; BMP4: bone morphogenetic protein 4; CD44: cluster of differentiation 44; CHAT: choline acetyltransferase; CHR: chromosome; CLDN4: claudin-4; ETS1: v-ets avian erythroblastosis virus E26 oncogene homolog 1; FGFR3: fibroblast growth factor receptor 3; FRZB: frizzled-related protein; FUT4: fucosyltransferase IV; IL18: interleukin 18; ITGB7: intergrin, beta 7; JAK3: janus kinase 3; MAP4K1: mitogen-activated protein kinase kinase kinase kinase 1; MAPK10: mitogen-activated protein kinase 10; PGLYRP2: peptidoglycan recognition protein 2; PIP5K1C: phosphatidylinositol-4-phosphate 5-kinase, type I, gamma; PLCB2: phospholipase C, beta 2; PRKAR1B: protein kinase, cAMP-dependent, regulatory, type I, beta; RIMS1: regulating synaptic membrane exocytosis 1; SH2D3C: SH2 domain containing 3C; SPI1: spleen focus forming virus (SFFV) proviral integration oncogene; STAB1: stabilin 1; TRIP6: thyroid hormone receptor interactor 6; TSS: transcription start site; UCSC: University of California Santa Cruz; UTR: untranslated region.
*Δβ indicates the magnitude of mean methylation difference between control group and treatment group.
**Negative value indicates the reduced methylation level in treatment group compared with control group.

Table III mRNA expression profile from a subset of differentially methylated EVT mobility-related genes.

Gene name	mRNA fold change (IL-15-EVT/CTL EVT)	P-value	mRNA fold change (HF-dNK-EVT/CTL EVT)	P-value
BMP4	0.75	0.0635	0.48*	0.0085
CLDN4	1.02	0.8692	0.79	0.0031
FGFR3	0.92	0.1522	0.55	0.0000
FUT4	0.90	0.0711	0.69	0.0021
IL18	1.04	0.2838	1.40	0.7875
ITGB7	1.46	0.2186	14.42**	0.0118
JAK3	1.36	0.1533	2.02	0.0405
PIP5K1C	1.01	0.9383	1.10	0.5799
PRKAR1B	1.15	0.5081	0.71	0.0212
TRIP6	1.23	0.3207	0.70	0.0477

CTL, control.
*Number smaller than 1 indicates the reduced mRNA expression in treatment group compared with control.
**Number bigger than 1 indicates the increased mRNA expression in treatment group compared with control.

methylation across gene regions were entered into the IPA software. Among them, 324 CpG sites across 275 individual genes were mapped to the IPA database and underwent core analysis. The top 5 associated network functions and top 5 molecular and cellular functions that were over-represented in the data set, along with the number of genes assigned to each category, are listed in Table I. The network composition and top four networks were centered on key cellular proteins p38

mitogen-activated protein kinase (P38 MAPK), phosphoinositide 3-kinase (PI3K)/protein kinase B (AKT) and extracellular signal-regulated protein kinase 1 and 2 (ERK1/2), and hence were involved in critical cellular functions of cell-to-cell signaling and interaction, cell proliferation and cell mobility. Two representative networks out of the top 5 are shown in Fig. 2. The primary molecular and cellular functions of genes derived from HF-dNK-treated EVT were associated with cellular
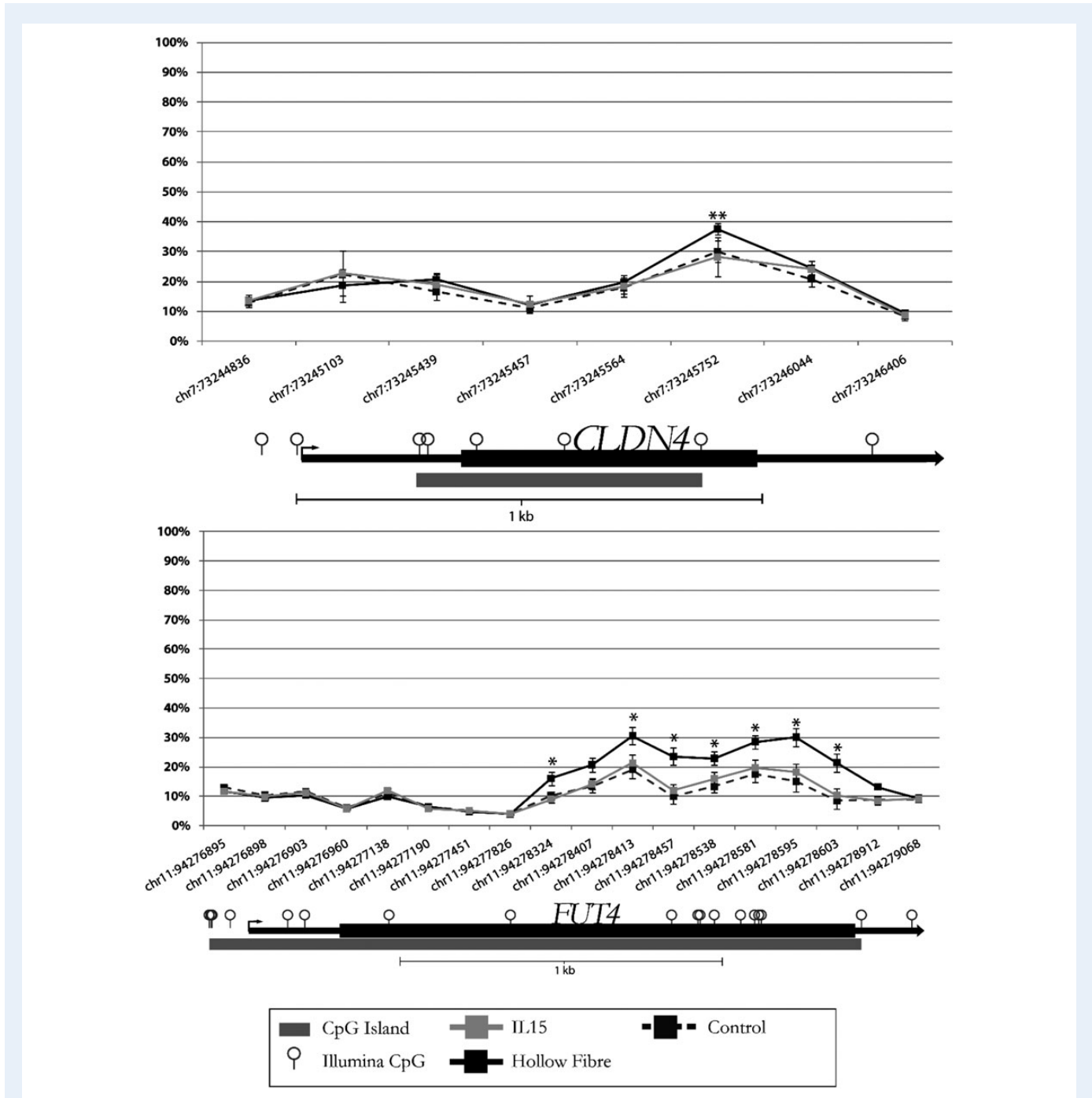

Figure 3 *CLDN4* and *FUT4* methylation probe allocation in Illumina HumanMethylation450 array (450 array). *CLDN4* and *FUT4* DNA methylation probes in 450 array were targeting multiple CpG sites across whole gene regions. The CpG sites with significantly increased CpG methylation were located in the enhancer region (or first Exon). CLDN4 (chr7: 73245752); FUT4 (chr11: 94278324-chr11: 94278603) *$P < 0.001$; **$P < 0.01$.

development, cellular growth and proliferation, cell signaling and inter-action, and especially with cellular movement, which is in line with our previous finding that HF-dNK regulate EVT migration and invasion (Hu *et al.*, 2006). Exposure of HF-dNK to EVT resulted in DNA methylation alteration of 23 cell mobility genes (Table II). Of these genes, 19 were associated with hypermethylated CpGs and the remainder were asso-ciated with hypomethylated CpGs. The top 50 differentially hyper-methylated CpGs and all hypomethylated CpGs which mapped to the IPA database and were associated with non-mobility genes by IPA are listed in Supplementary Tables SI and SII, respectively. The genes assigned to the categories with other molecular and cellular functions are listed in Supplementary Table SIII.

mRNA expression profile for a subset of mobility-related genes and follow-up of the *CLDN4* and *FUT4* methylation changes with bisulfite pyrosequencing

The mRNA expression profile of EVT from explants was carried out for a subset of genes from the mobility list (Table II) and normalized by GAPDH (Table III). The house-keeping gene ACTB confirmed the results obtained by normalizing data with GAPDH (data not shown). The differentially hypermethylated CpGs for *BMP4*, *FGFR3*, *JAK3*, *ITGB7*, *PRKAR1B*, *PIP5K1C* and *TRIP6* were located in the gene-body, and their mRNA expression levels were decreased for *BMP4*, *FGFR3*,

PRKARIB and *TRIP6*, increased for *JAK3* and *ITGB7* or did not reach stat-istical significance for *PIP5K1C*. The hypomethylated CpG for *IL-18* was in transcription start site (TSS) 200, and its mRNA expression showed a trend of increased expression but did not reach statistical significance. The hypermethylated CpGs for *CLDN4* and *FUT4* were in the first exon which overlapped with a putative enhancer (Fig. 3) and their mRNA expression levels were reduced (Table III).

In the subset of genes, two significant sites were identified for follow-up study due to their association with functionally relevant genes. CLDN4 is a member of a large family of transmembrane proteins that are essential in the formation and maintenance of tight junctions. Clau-dins influence a wide variety of processes including cell signaling, prolifer-ation, differentiation, trafficking and polarity (Escudero-Esparza *et al.*, 2011). FUT4 is a member of a family of genes involved in various biologic-al processes, including cell adhesion, lymphocyte homing, embryo-fetal development, tumor progression, etc. (Cailleau-Thomas *et al.*, 2000; Julien *et al.*, 2011; Padro *et al.*, 2011; Yang *et al.*, 2013). Pyrosequencing results confirmed an increase in DNA methylation at each candidate CpG and adjacent CpGs for HF-dNK-treated EVT, but not IL-15, for *CLDN4* and *FUT4* (Supplementary Fig. S2). EVT harvested from villous explant cultures had decreased *CLDN4* and *FUT4* protein expression as measured by flow cytometry (Fig. 4a and b) as well as decreased mRNA expression as detected by RT-qPCR (Table III). These data indi-cate that *CLDN4* and *FUT4* expression is inversely correlated with DNA methylation at the exon 1 enhancers.
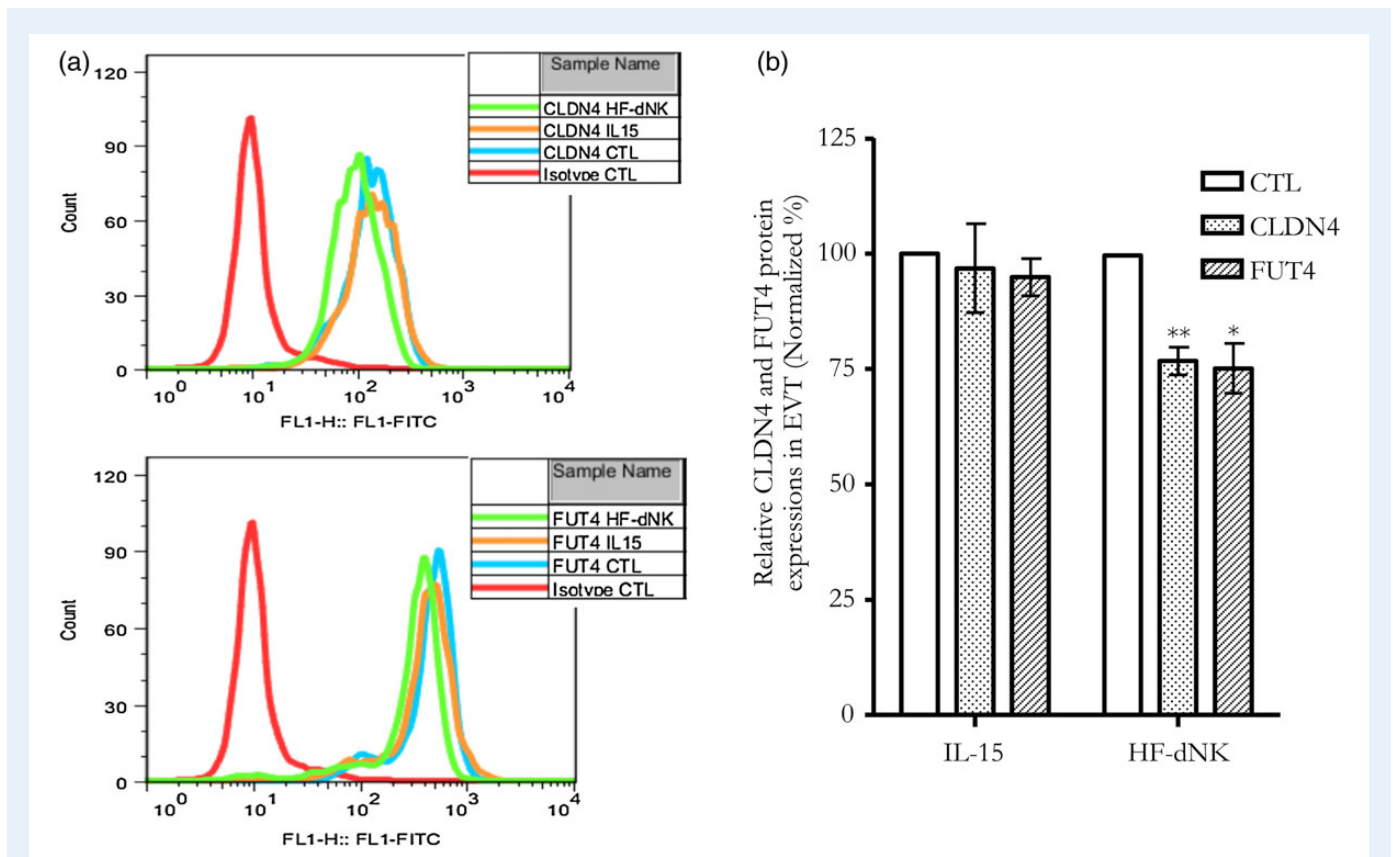

Figure 4 CLDN4 and FUT4 protein expressions in EVT from explant culture. (**a**) CLDN4 and FUT4 protein expressions measured by flow cytometry; (**b**) mean density of flow cytometry for CLDN4 and FUT4. *$P < 0.001$; **$P < 0.01$. CLDN4 and FUT4 protein expressions were reduced by exposure to dNK-HF but not IL-15. CTL: control.
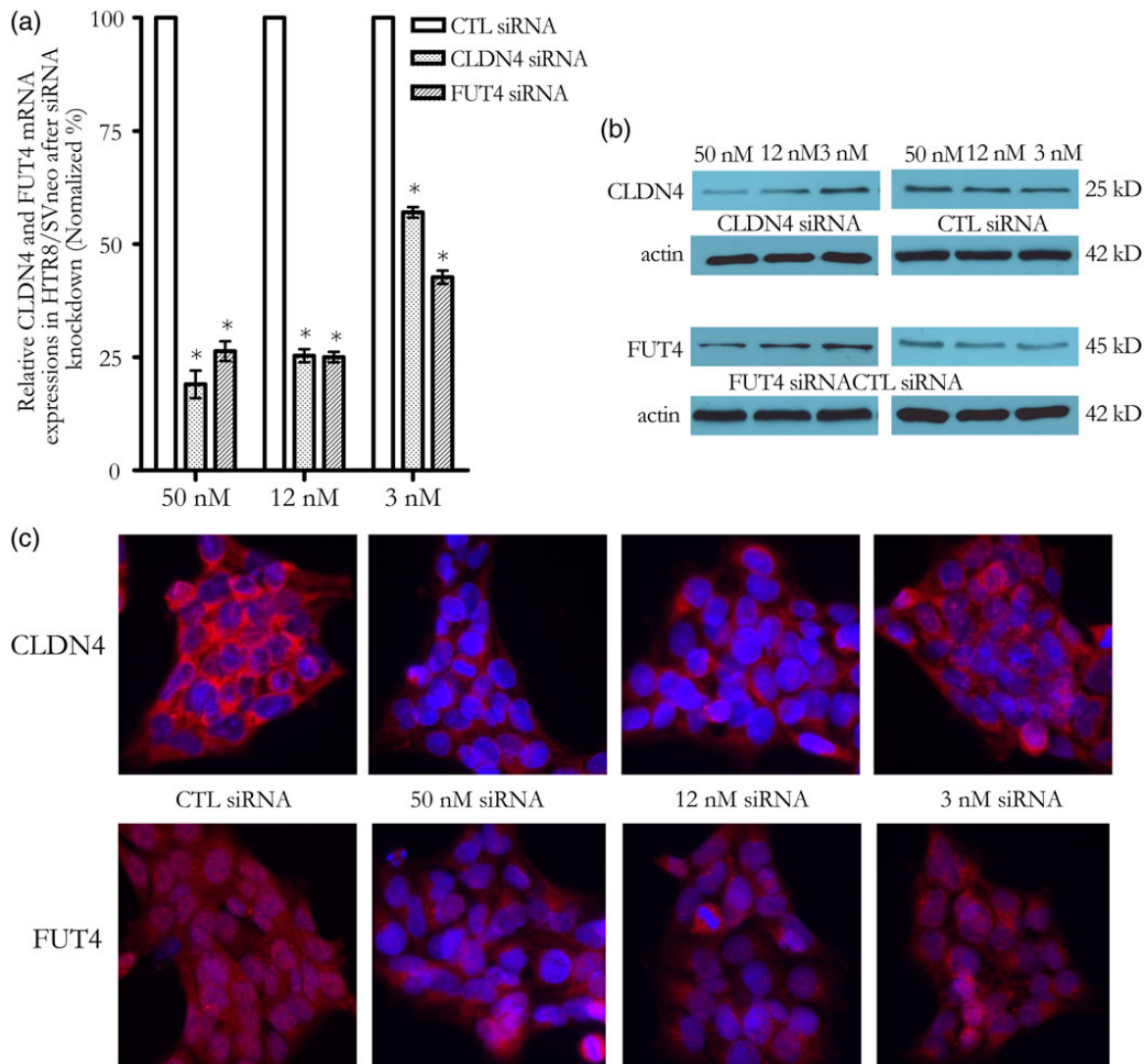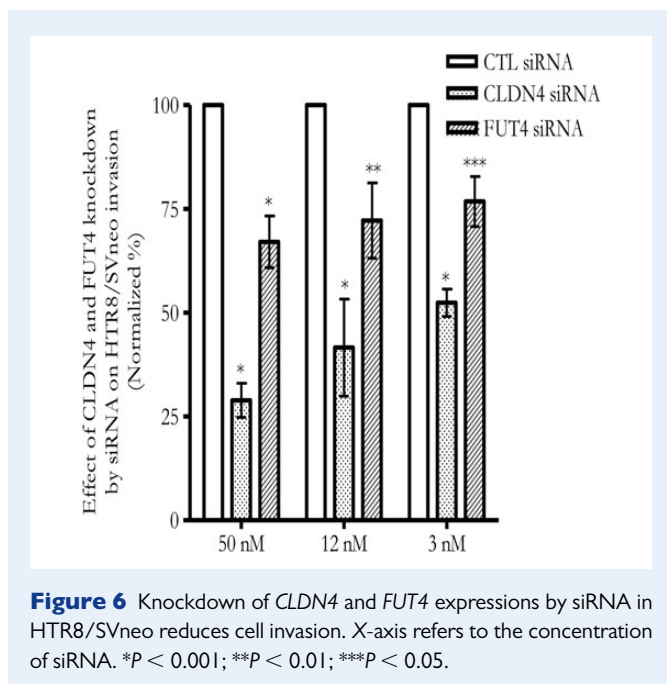
Figure 5 CLDN4 and FUT4 mRNA and protein expressions in HTR8/SVneo cells. (**a**) CLDN4 and FUT4 mRNA expressions were reduced by small interfering RNA (siRNA) transfection as measured by qPCR. *$P < 0.001$; (**b** and **c**) CLDN4 and FUT4 protein expressions were reduced by siRNA transfection as measured by western blot (b) and immunocytochemistry staining (c). CLDN4 displayed a primary membrane staining, and FUT4 was a primary cytoplasmic staining. Blue color showed the 4′,6-Diamidino-2-phenylindole (DAPI) nuclear staining; Red color was CLDN4 or FUT4 protein staining. Magnification of images: ×400.

CLDN4 and FUT4 knockdown by siRNA in the EVT cell line HTR8/SVneo reduces cell invasion and alters MMP-2 and/or MMP-9 expression

To determine the role of *CLDN4* and *FUT4* in EVT, siRNA was introduced into the EVT cell line, HTR8/SVneo, to knock down their expression level. Knockdown efficiency was confirmed by RT-qPCR. At 48 h after transfection, *CLDN4* and *FUT4* siRNA, but not control siRNA, at concentrations as low as 12 nM showed >70% *CLDN4* mRNA and *FUT4* mRNA reduction as detected by RT-qPCR which was normalized by GAPDH (Fig. 5a) and ACTB (data not shown). CLDN4 and FUT4 protein expression was reduced 72–96 h after transfection, as detected by western blot (Fig. 5b) and immunocytochemistry staining (Fig. 5c). The CLDN4 antibody stained a primary membrane protein and FUT4 antibody stained a primary cytoplasmic protein in HTR8/SVneo cells (Fig. 5c). Knockdown of *CLDN4* and *FUT4* was accompanied by a reduction of HTR8/SVneo invasion (Fig. 6). Co-transfection with *CLDN4* siRNA and *FUT4* siRNA can knockdown *CLDN4* and *FUT4* mRNA expression as effectively as *CLDN4* siRNA or *FUT4* siRNA transfection alone. However a further reduction of invasion compared with *CLDN4* or *FUT4* transfection alone was not observed (data not shown). Active MMP-2 and MMP-9 as well as total MMP-2 and MMP-9 were reduced following *CLDN4* knocking down (Fig. 7a and b). In the case of *FUT4*

Figure 6 Knockdown of *CLDN4* and *FUT4* expressions by siRNA in HTR8/SVneo reduces cell invasion. *X*-axis refers to the concentration of siRNA. *$P < 0.001$; **$P < 0.01$; ***$P < 0.05$.

knockdown, active MMP-2 and total MMP-2 changes did not reach significance (Fig. 7c); active MMP-9 was reduced while total MMP-9 was increased (Fig. 7d).

Discussion

In this study, we observed alterations of DNA methylation in EVT exposed to dNK using a large-scale microarray approach and, for two selected genes, demonstrated corresponding changes in mRNA and protein expression. Through secreted soluble factors, such as growth factors, chemokines and cytokines (Clark *et al.*, 1994; Vigano *et al.*, 2001; Hanna *et al.*, 2006; Hu *et al.*, 2006, 2008; Lash *et al.*, 2006; Pitman *et al.*, 2013), dNK regulate EVT phenotypic traits, such as cell invasion, by affecting protein expression; this altered expression can be associated with altered DNA methylation (Fig. 1). Using the 450 k array, we observed no global DNA methylation level change by HF-dNK treatment compared with medium control; however we did see a small percentage of CpG loci which were altered with HF-dNK exposure (Fig. 1). Many of these loci were located on genes which are in critical cell signaling pathways such as p38 MAPK, PI3K/AKT and ERK1/2 pathways. *CLDN4* and *FUT4*, the two follow-up genes in the current study, were involved in ERK1/2 and AKT pathways (Fig. 2a and b). The results indicate how dNK may modulate EVT functions. IL-15 was applied in HF-dNK when co-culturing with explants to maintain dNK viability and proliferation. There were 73 CpG loci methylation alterations using our cut-off in IL-15-treated EVT. Among them, there were only 5 loci in common with HF-dNK-treated EVT, indicating the minimal impact of IL-15 on EVT DNA methylation by HF-dNK.
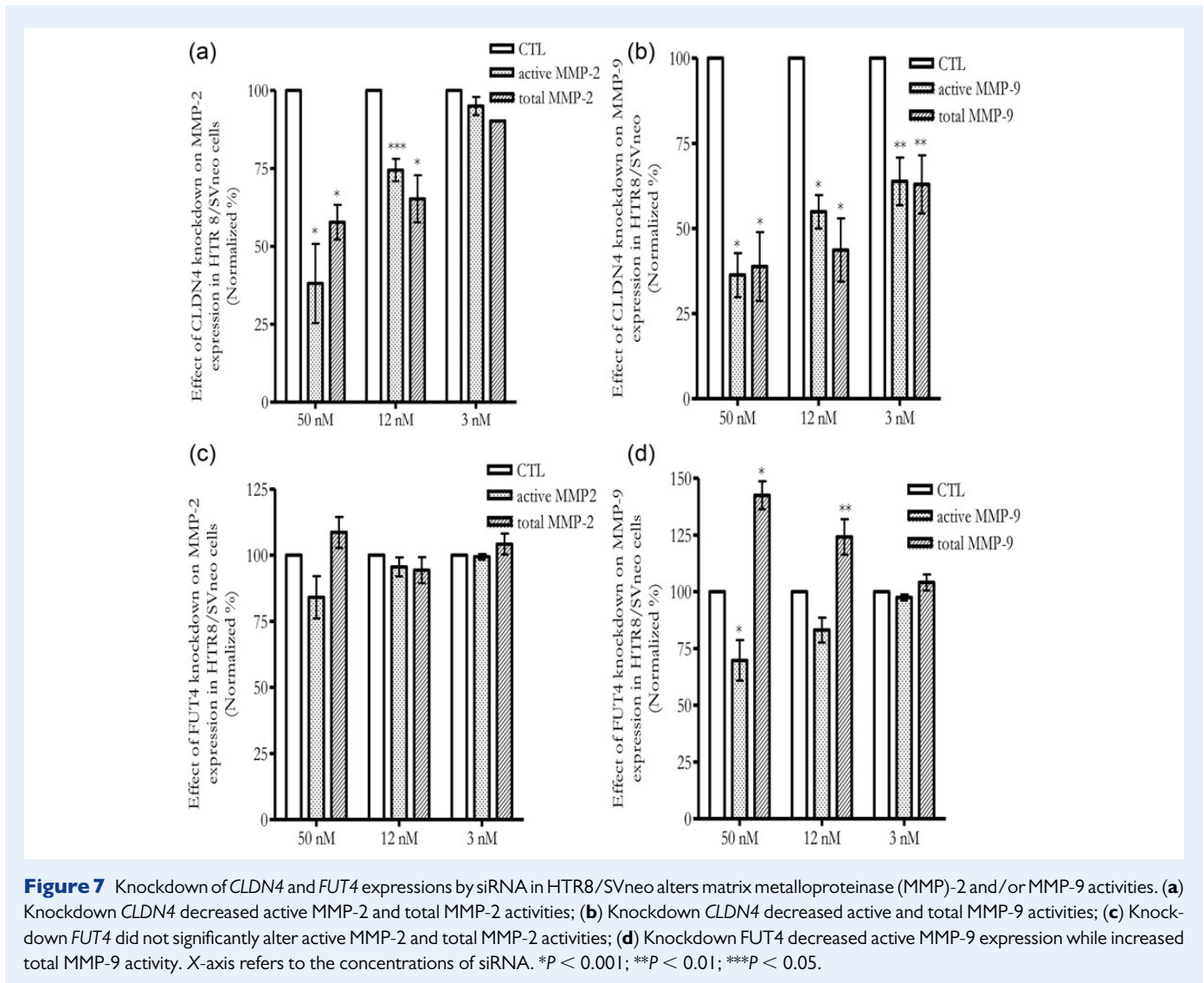
Changes in DNA methylation can cause changes in gene expression or changes in gene expression can drive changes in DNA methylation. While we can only speculate about the mechanism, as invasive EVT in decidua are non-dividing cells hence changes to DNA methylation must be replication-independent. DNA methylation is accomplished and maintained by a family of enzymes called DNA methyltransferases

(DNMTs). DNMTs can be regulated by steroid hormones, growth factors, cell cycle regulators, viruses and cytokines (Logan *et al.*, 2013). dNK produce a number of soluble factors which can potentially modulate DNMTs expression, leading to EVT DNA methylation alteration. IL-6 was reported to increase DNMT1 expression and epigenetically regulate the expression of several genes in cholangiocarcinoma (Braconi *et al.*, 2010); TGF-β1 modulated DNMTs expression and TGF-β signaling is directly and indirectly related to all DNA methylated genes detected in prostate cancer (Zhang *et al.*, 2011; Lee *et al.*, 2012); TNF-α reduced DNA methylation in chondrocytes via inhibiting DNMT1 expression (Hashimoto *et al.*, 2009). While active DNA methylation may result from DNMT expression and activity changes, some changes to DNA methylation may also occur as a consequence of chromatin changes resulting from protein binding associated with gene expression.

The DNA methylation profiling of EVT interacting with HF-dNK identified a list of EVT mobility-related genes (Table II). The roles of some genes from the list has been studied in oncology but not yet explored in trophoblast biology, as is the case for *CLDN4* and *FUT4* investigated in the current study. Other examples include *CD44*, *BMP4*, *TRIP6* and phospholipase C, beta 2 (*PCLB2*) (Bertagnolo *et al.*, 2007; Guo *et al.*, 2012; Idowu *et al.*, 2012; Grunewald *et al.*, 2013), and a few kinases such as mitogen-activated protein kinase kinase kinase kinase 1 (*MAP4K1*), mitogen-activated protein kinase 10 (*MAPK10*), *PIP5K1C* and *FGFR3* which are located in MAP kinase, phosphoinositide and FGFR cell signaling pathways involving in cell proliferation, migration and invasion. The result here implies that multiple cell mobility regulatory genes may be involved in dNK-mediated EVT migration and invasion modulation.

The relationship between DNA methylation and expression is complex and related in part to the genomic location of the methylated elements. DNA methylation in the promoter region is often associated with down-regulation of gene expression (Wong *et al.*, 2010). DNA methylation in the first exon may also be linked to transcriptional silence (Brenet *et al.*, 2011). In contrast, gene-body DNA methylation tends to be positively correlated with gene expression levels (Rauch *et al.*, 2009). A recent study has shown that the relationship between gene-body DNA methylation and expression level is non-monotonic and bell-shaped (Jjingo *et al.*, 2012). The mRNA expression level of individual genes observed in Table III was not always correlated with DNA methylation level. There is however not expected to be a one-to-one correspondence with gene expression and many other factors may be relevant for regulating gene expression. For example, EVT gene expression may be regulated by DNA-binding transcription factors, or stimulated by dNK-secreted growth factors, chemokines and cytokines (Clark *et al.*, 1994; Vigano *et al.*, 2001; Hanna *et al.*, 2006; Hu *et al.*, 2006, 2008; Lash *et al.*, 2006; Pitman *et al.*, 2013), or through dNK-EVT interaction via cell surface receptors (Wallace *et al.*, 2012). The observed mRNA expression may have been an overall effect of dNK-derived soluble factors, either from epigenetic modification, including DNA methylation, or transcriptional, post-transcriptional and translational regulation.

CLDN4 expression is frequently disrupted in various tumors (Michl *et al.*, 2003; Agarwal *et al.*, 2005; Boireau *et al.*, 2007; Litkouhi *et al.*, 2007; Kwon *et al.*, 2011), and is often inversely correlated with DNA methylation (Litkouhi *et al.*, 2007; Kwon *et al.*, 2011). Elevated *CLDN4* expression level has been shown to either decrease (Michl *et al.*, 2003)

Figure 7 Knockdown of *CLDN4* and *FUT4* expressions by siRNA in HTR8/SVneo alters matrix metalloproteinase (MMP)-2 and/or MMP-9 activities. (**a**) Knockdown *CLDN4* decreased active MMP-2 and total MMP-2 activities; (**b**) Knockdown *CLDN4* decreased active and total MMP-9 activities; (**c**) Knockdown *FUT4* did not significantly alter active MMP-2 and total MMP-2 activities; (**d**) Knockdown FUT4 decreased active MMP-9 expression while increased total MMP-9 activity. *X*-axis refers to the concentrations of siRNA. *$P < 0.001$; **$P < 0.01$; ***$P < 0.05$.

or increase (Agarwal et al., 2005; Litkouhi et al., 2007; Lee et al., 2008) tumor migration or invasion depending on cell type. MMP-2/MMP-9 level and activity appear to be regulated by *CLDN4* (Oku et al., 2006; Lee et al., 2008). CLDN4 expression is regulated by the MAPK signaling pathway (Carrozzino et al., 2009). CLDN4 may modulate the activation of PI3K/AKt signaling pathway via altering Akt phosphorylation, cellular PIP3 content and PI3K activity (Lin et al., 2013), which subsequently leads to activity changes of MMPs (Rychahou et al, 2004; Wang et al, 2004). These results indicate that CLDN4 mediates the alteration of MMPs expression and activity potentially through MAPK and PI3K signaling pathways. We observed that knocking down *CLDN4* in HTR8/SVneo reduced cell invasion, which was probably associated with reduced MMP-2 and MMP-9 activity (Fig. 7a and b). The lowered level of active MMP-2 and MMP-9 in *CLDN4* knocked down HTR8/SVneo might reflect the reduced level of total MMP-2 and MMP-9.

FUT4 expression is increased in various tumor cells (Julien et al., 2011; Padro et al., 2011; Li et al., 2012) and regulated by promoter methylation (Li et al., 2012). In breast cancer cells, *FUT4* induced activation of

phosphatidylinositol 3 kinase (PI3K)/AKT, and inactivation of glycogen synthase kinase 3 beta (GSK3β) and nuclear translocation of nuclear factor of kappa light polypeptide gene enhancer in B-cells (NF-κB), resulting in increased Snail and MMP-9 expression and greater cell mobility (Yang et al., 2013). FUT4 also promotes cancer cell proliferation through activating MAPK and PI3K/AKT signaling pathways (Yang et al., 2010). The alterations of PI3K/AKT and MAPK pathways are tightly linked to the activity changes of MMPs as described (Rychahou et al., 2004; Wang et al., 2004). We showed that *FUT4* knockdown in HTR8/SVneo cells by siRNA reduced cell invasion, which might be related to the reduction of MMP-9 activity although total MMP-9 expression was increased (Fig. 7d), the same phenomenon we observed previously in EVT interacting with dNK in an explant culture model (Hu et al., 2006). *FUT4* knockdown in HTR8/SVneo might impact the activation process of MMP-9. The study in Age-related Macular Degeneration (AMD) patients found the reduction of fully active 84-kDa MMP-9 by observing the co-existence of a partially active 88-kDa transitional intermediate MMP-9, which implies the existence of problems with the

MMP-9 cellular activation process (Hussain *et al.*, 2011). The phenomenon, however, needs to be studied in HTR8/SVneo cells. Our previous study demonstrated that dNK restricted EVT migration and invasion, which was associated with alterations of MMP-2 and MMP-9 expression and activity (Hu *et al.*, 2006). dNK modulated EVT mobility-related gene expression through methylation, with *CLDN4* and *FUT4* as examples, which might indirectly lead to changes in expression and activity of MMP-2 and/or MMP-9.

The present study has several limitations. This study was limited by the small sample size, and thus lacked the power for genome-wide correction for multiple comparisons. However, the power was strengthened by the use of genetically matched samples in our comparisons. A larger sample size would be required to draw more certain conclusions in terms of actual number of loci affected and degree of change. The follow-up studies for selected candidates, *CLDN4* and *FUT4*, focused on an EVT cell line due to limited access to primary EVT. HTR8/SVneo is an immortalized EVT cell line that inherits the features of primary EVT (Graham *et al.*, 1993).

Despite the limitations, these data might suggest a regulatory effect of dNK on trophoblast, at least in part by altering gene expression through DNA methylation. *CLDN4* and *FUT4* are examples of genes that are regulated by dNK and associated with methylation alteration. In addition to changes in expression of *CLDN4* and *FUT4*, the expression of downstream molecules MMP-2 and/or MMP-9 is further modulated, which ultimately leads to changes in the function of EVT such as EVT migration and invasion. Further study of other EVT mobility-related candidate genes would provide a broad spectrum of data regarding the regulation of trophoblast migration and invasion.

Supplementary data

Supplementary data are available at http://molehr.oxfordjournals.org/.

Acknowledgements

Authors' roles

Y.H., J.D.B., R.K.C.Y. and P.v.D. conceived and designed the experiments, Y.H., J.D.B. and R.K.C.Y. performed the experiments, Y.H., J.D.B., W.P.R. and P.v.D. analyzed the data and Y.H., J.D.B., W.P.R. and P.v.D. wrote the paper.

Funding

Conflict of interest

None declared.

References

Agarwal R, D'Souza T, Morin PJ. Claudin-3 and claudin-4 expression in ovarian epithelial cells enhances invasion and is associated with increased matrix metalloproteinase-2 activity. *Cancer Res* 2005; **65**:7378–7385.

Bertagnolo V, Benedusi M, Brugnoli F, Lanuti P, Marchisio M, Querzoli P, Capitani S. Phospholipase C-beta 2 promotes mitosis and migration of human breast cancer-derived cells. *Carcinogenesis* 2007;**28**:1638–1645.

Blair JD, Yuen RK, Lim BK, McFadden DE, von Dadelszen P, Robinson WP. Widespread DNA hypomethylation at gene enhancer regions in placentas associated with early-onset pre-eclampsia. *Mol Hum Reprod* 2013;**19**:697–708.

Boireau S, Buchert M, Samuel MS, Pannequin J, Ryan JL, Choquet A, Chapuis H, Rebillard X, Avances C, Ernst M *et al.* DNA-methylation-dependent alterations of claudin-4 expression in human bladder carcinoma. *Carcinogenesis* 2007;**28**:246–258.

Braconi C, Huang N, Patel T. MicroRNA-dependent regulation of DNA methyltransferase-1 and tumor suppressor gene expression by interleukin-6 in human malignant cholangiocytes. *Hepatology* 2010; **51**:881–890.

Brenet F, Moh M, Funk P, Feierstein E, Viale AJ, Socci ND, Scandura JM. DNA methylation of the first exon is tightly linked to transcriptional silencing. *PLoS One* 2011;**6**:e14524.

Burrows TD, King A, Loke YW. Trophoblast migration during human placental implantation. *Hum Reprod Update* 1996;**2**:307–321.

Cailleau-Thomas A, Coullin P, Candelier JJ, Balanzino L, Mennesson B, Oriol R, Mollicone R. FUT4 and FUT9 genes are expressed early in human embryogenesis. *Glycobiology* 2000;**10**:789–802.

Carrozzino F, Pugnale P, Féraille E, Montesano R. Inhibition of basal p38 or JNK activity enhances epithelial barrier function through differential modulation of claudin expression. *Am J Physiol Cell Physiol* 2009; **297**:C775–C787.

Clark DA, Vince G, Flanders KC, Hirte H, Starkey P. CD56+ lymphoid cells in human first trimester pregnancy decidua as a source of novel transforming growth factor-beta 2-related immunosuppressive factors. *Hum Reprod* 1994;**9**:2270–2277.

Damsky CH, Fitzgerald ML, Fisher SJ. Distribution patterns of extracellular matrix components and adhesion receptors are intricately modulated during first trimester cytotrophoblast differentiation along the invasive pathway, in vivo. *J Clin Invest* 1992;**89**:210–222.

Eastabrook G, Hu Y, von Dadelszen P. The role of decidual natural killer cells in normal placentation and in the pathogenesis of preeclampsia. *J Obstet Gynaecol Can* 2008;**30**:467–476.

Eastabrook G, Hu Y, Tan R, Dutz JP, Maccalman CD, von Dadelszen P. Decidual NK cell-derived conditioned medium (dNK-CM) mediates VEGF-C secretion in extravillous cytotrophoblasts. *Am J Reprod Immunol* 2012;**67**:101–111.

Escudero-Esparza A, Jiang WG, Martin TA. The Claudin family and its role in cancer and metastasis. *Front Biosci (Landmark Ed)* 2011;**16**:1069–1083.

Fukushima K, Miyamoto S, Tsukimori K, Kobayashi H, Seki H, Takeda S, Kensuke E, Ohtani K, Shibuya M, Nakano H. Tumor necrosis factor and vascular endothelial growth factor induce endothelial integrin repertories, regulating endovascular differentiation and apoptosis in a human extravillous trophoblast cell line. *Biol Reprod* 2005;**73**:172–179.

Graham CH, Hawley TS, Hawley RG, MacDougall JR, Kerbel RS, Khoo N, Lala PK. Establishment and characterization of first trimester human trophoblast cells with extended lifespan. *Exp Cell Res* 1993; **206**:204–211.

Grunewald TG, Willier S, Janik D, Unland R, Reiss C, Prazeres da Costa O, Buch T, Dirksen U, Richter GH, Neff F *et al.* The Zyxin-related protein thyroid receptor interacting protein 6 (TRIP6) is overexpressed in

Ewing's sarcoma and promotes migration, invasion and cell growth. *Biol Cell* 2013;**105**:535−547.

Guo D, Huang J, Gong J. Bone morphogenetic protein 4 (BMP4) is required for migration and invasion of breast cancer. *Mol Cell Biochem* 2012;**363**:179−190.

Hamilton JP. Epigenetics: principles and practice. *Dig Dis* 2011;**29**:130−135.

Hanna J, Goldman-Wohl D, Hamani Y, Avraham I, Greenfield C, Natanson-Yaron S, Prus D, Cohen-Daniel L, Arnon TI, Manaster I et al. Decidual NK cells regulate key developmental processes at the human fetal-maternal interface. *Nat Med* 2006;**12**:1065−1074.

Hashimoto K, Oreffo ROC, Gibson MB, Goldring MB, Roach HI. DNA demethylation at specific CpG sites in the *IL1B* promoter in response to inflammatory cytokines in human articular chondrocytes. *Arthritis Rheum* 2009;**60**:3303−3313.

Hu Y, Dutz JP, MacCalman CD, Yong P, Tan R, von Dadelszen P. Decidual NK cells alter *in vitro* first trimester extravillous cytotrophoblast migration: a role for IFN-gamma. *J Immunol* 2006;**177**:8522−8530.

Hu Y, Tan R, MacCalman CD, Eastabrook G, Park SH, Dutz JP, von Dadelszen P. IFN-gamma-mediated extravillous trophoblast outgrowth inhibition in first trimester explant culture: a role for insulin-like growth factors. *Mol Hum Reprod* 2008;**14**:281−289.

Hu Y, Eastabrook G, Tan R, MacCalman CD, Dutz JP, von Dadelszen P. Decidual NK cell-derived conditioned medium enhances capillary tube and network organization in an extravillous cytotrophoblast cell line. *Placenta* 2010;**31**:213−221.

Hussain AA, Lee Y, Zhang JJ, Marshall J. Disturbed matrix metalloproteinase activity of Bruch's membrane in age-related macular degeneration. *Invest Ophthalmol Vis Sci* 2011;**52**:4459−4466.

Idowu MO, Kmieciak M, Dumur C, Burton RS, Grimes MM, Powers CN, Manjili MH. CD44(+)/CD24(-/low) cancer stem/progenitor cells are more abundant in triple-negative invasive breast carcinoma phenotype and are associated with poor outcome. *Hum Pathol* 2012;**43**:364−373.

Jjingo D, Conley AB, Jordan IK. On the presence and the role of human gene-body DNA methylation. *Oncotarget* 2012;**3**:462−474.

Julien S, Ivetic A, Grigoriadis A, QiZe D, Burford B, Sproviero D, Picco G, Gillett C, Papp SL, Schaffer L et al. Selectin ligand sialyl-Lewis x antigen drives metastasis of hormone-dependent breast cancers. *Cancer Res* 2011;**71**:7683−7693.

Karmakar S, Das C. Regulation of trophoblast invasion by IL-1 beta and TGF-beta 1. *Am J Reprod Immunol* 2002;**48**:210−219.

Knofler M. Critical growth factors and signalling pathways controlling human trophoblast invasion. *Int J Dev Biol* 2010;**54**:269−280.

Kwon MJ, Kim SH, Jeong HM, Jung HS, Kim SS, Lee JE, Gye MC, Erkin OC, Koh SS, Choi YL et al. Claudin-4 overexpression is associated with epigenetic derepression in gastric carcinoma. *Lab Invest* 2011;**91**:1652−1667.

Lash GE, Otun HA, Innes BA, Bulmer JN, Searle RF, Robson SC. Inhibition of trophoblast cell invasion by TGFB1, 2, and 3 is associated with a decrease in active proteases. *Biol Reprod* 2005;**74**:403−409.

Lash GE, Schiessl B, Kirkley M, Innes BA, Cooper A, Searle RF, Robson SC, Bulmer JN. Expression of angiogenic growth factors by uterine natural killer cells during early pregnancy. *J Leukoc Biol* 2006;**80**:572−580.

Lee LY, Wu CM, Wang CC, Yu JS, Liang Y, Huang KH, Lo CH, Hwang TL. Expression of matrix metalloproteinases MMP-2 and MMP-9 in gastric cancer and their relation to claudin-4 expression. *Histol Histopathol* 2008;**23**:515−521.

Lee C, Zhang Q, Zi X, Dash A, Soares MB, Rahmatpanah F, Jia Z, McClelland M, Mercola D. TGF-β mediated DNA methylation in prostate cancer. *Transl Androl Urol* 2012;**1**:78−88.

Li H, Tong S, Liu J, Han L, Yang X, Hou H, Yan Q, Wang XQ. Differential fucosyltransferase IV expression in squamous carcinoma cells is regulated by promoter methylation. *Cell Mol Biol Lett* 2012;**17**:206−216.

Lin X, Shang X, Manorek G, Howell SB. Regulation of the epithelial-mesenchymal transition by Claudin-3 and Claudin-4. *PLoS One* 2013;**8**:e67496. doi:10.1371/journal.pone.0067496.

Litkouhi B, Kwong J, Lo CM, Smedley JG, McClane BA, Aponte M, Gao Z, Sarno JL, Hinners J, Welch WR et al. Claudin-4 overexpression in epithelial ovarian cancer is associated with hypomethylation and is a potential target for modulation of tight junction barrier function using a C-terminal fragment of Clostridium perfringens enterotoxin. *Neoplasia* 2007;**9**:304−314.

Logan PC, Mitchell MD, Lobie PE. DNA methyltransferases and TETs in the regulation of differentiation and invasiveness of extra-villous trophoblasts. *Front Genet* 2013;**4**:265.

Michl P, Barth C, Buchholz M, Lerch MM, Rolke M, Holzmann KH, Menke A, Fensterer H, Giehl K, Lohr M et al. Claudin-4 expression decreases invasiveness and metastatic potential of pancreatic cancer. *Cancer Res* 2003;**63**:6265−6271.

Mohtat D, Susztak K. Fine tuning gene expression: the epigenome. *Semin Nephrol* 2010;**30**:468−476.

Oku N, Sasabe E, Ueta E, Yamamoto T, Osaki T. Tight junction protein claudin-1 enhances the invasive activity of oral squamous cell carcinoma cells by promoting cleavage of laminin-5 gamma2 chain via matrix metalloproteinase (MMP)-2 and membrane-type MMP-1. *Cancer Res* 2006;**66**:5251−5257.

Padro M, Cobler L, Garrido M, de Bolos C. Down-regulation of FUT3 and FUT5 by shRNA alters Lewis antigens expression and reduces the adhesion capacities of gastric cancer cells. *Biochim Biophys Acta* 2011;**1810**:1141−1149.

Pang ZJ, Zhou JG, Huang LP. Interleukin-10 may participate in regulating trophoblast invasion in human placentae throughout gestation. *Am J Reprod Immunol* 2008;**60**:19−25.

Pitman H, Innes BA, Robson SC, Bulmer JN, Lash GE. Altered expression of interleukin-6, interleukin-8 and their receptors in decidua of women with sporadic miscarriage. *Hum Reprod* 2013;**28**:2075−2086.

Rauch TA, Wu X, Zhong X, Riggs AD, Pfeifer GP. A human B cell methylome at 100-base pair resolution. *Proc Natl Acad Sci USA* 2009;**106**:671−678.

Rychahou PG, Murillo C, Evers BM. Downregulation of the PI3k/Akt pathway leads to decreased invasion of the human colon cancer cells. *J Am Coll Surg* 2004;**199**:10 Supplement.

Vigano P, Gaffuri B, Somigliana E, Infantino M, Vignali M, Di Blasio AM. Interleukin-10 is produced by human uterine natural killer cells but does not affect their production of interferon-gamma. *Mol Hum Reprod* 2001;**7**:971−977.

Wallace AE, Fraser R, Cartwright JE. Extravillous trophoblast and decidual natural killer cells: a remodelling partnership. *Hum Reprod Update* 2012;**18**:458−471.

Wang L, Zhang ZG, Zhang RL, Gregg SR, Hozeska-Solgot A, LeTourneau Y, Wang Y, Chopp M. Matrix metalloproteinase 2 (MMP2) and MMP9 secreted by erythropoietin-activated endothelial cells promote neural progenitor cell migration. *J Neurosci* 2004;**26**:5996−6003.

Wong E, Li G, Huynh T, Tsirigos A, Ong CT, Low HM, Kin Sung KW, Rigoutsos I, Loving J, Wei CL. Dynamic changes in the human methylome during differentiation. *Genome Res* 2010;**20**:320−331.

Yagel S. The developmental role of natural killer cells at the fetal-maternal interface. *Am J Obstet Gynecol* 2009;**201**:344−350.

Yang XS, Liu S, Liu YJ, Liu JW, Liu TJ, Wang XQ, Yan Q. Overexpression of fucosyltransferase IV promotes A431 cell proliferation through activating MAPK and PI3K/Akt signaling pathways. *J Cell Physiol* 2010;**225**:612−619.

Yang X, Liu S, Yan Q. Role of fucosyltransferase IV in epithelial-mesenchymal transition in breast cancer cells. *Cell Death Dis* 2013;**4**:e735.

Yuen RK, Penaherrera MS, von Dadelszen P, McFadden DE, Robinson WP. DNA methylation profiling of human placentas reveals promoter

hypomethylation of multiple genes in early-onset preeclampsia. *Eur J Hum Genet* 2010;**18**:1006–1012.

Yuen RK, Chen B, Blair JD, Robinson WP, Nelson DM. Hypoxia alters the epigenetic profile in cultured human placental trophoblasts. *Epigenetics* 2013;**8**:192–202.

Zhang Q, Chen L, Helfand BT, Jang TL, Sharma V, Kozlowski J, Kuzel TM, Zhu LJ, Yang XJ, Javonovic B *et al.* TGF-b Regulates DNA Methyltransferase Expression in Prostate Cancer, Correlates with Aggressive Capabilities, and Predicts Disease Recurrence. *PLoS One* 2011;**6**:e25168. doi:10.1371/journal.pone.0025168.